Supplementary material for "Sensitivity of winter Arctic amplification in NorESM2"

Lise Seland Graff[1], Jerry Tjiputra[2,4], Ada Gjermundsen[1], Andreas Born[3,4], Jens Boldingh Debernard[1], Heiko Goelzer[2,4], Yan-Chun He[5,4], Petra Margaretha Langebroek[2,4], Aleksi Nummelin[2,6], Dirk Olivié[1], Øyvind Seland[1], Trude Storelvmo[7], Mats Bentsen[2,4], Chuncheng Guo[2,8], Andrea Rosendahl[1,3], Dandan Tao[3,4], Thomas Toniazzo[2,4], Camille Li[3,4], Stephen Outten[5,4], and Michael Schulz[1,7]

[1]Norwegian Meteorological Institute, Oslo, Norway
[2]NORCE Norwegian Research Centre AS, Bergen, Norway
[3]University of Bergen, Bergen, Norway
[4]Bjerknes Centre for Climate Research, Bergen, Norway
[5]Nansen Environmental and Remote Sensing Center, Bergen, Norway
[6]Finnish Meteorological Institute, Helsinki, Finland
[7]University of Oslo, Oslo, Norway
[8]National Centre for Climate Research, Danish Meteorological Institute, Copenhagen, Denmark

Correspondence: Lise Seland Graff (lise.s.graff@met.no)

This supplementary material contains additional figures and a table.

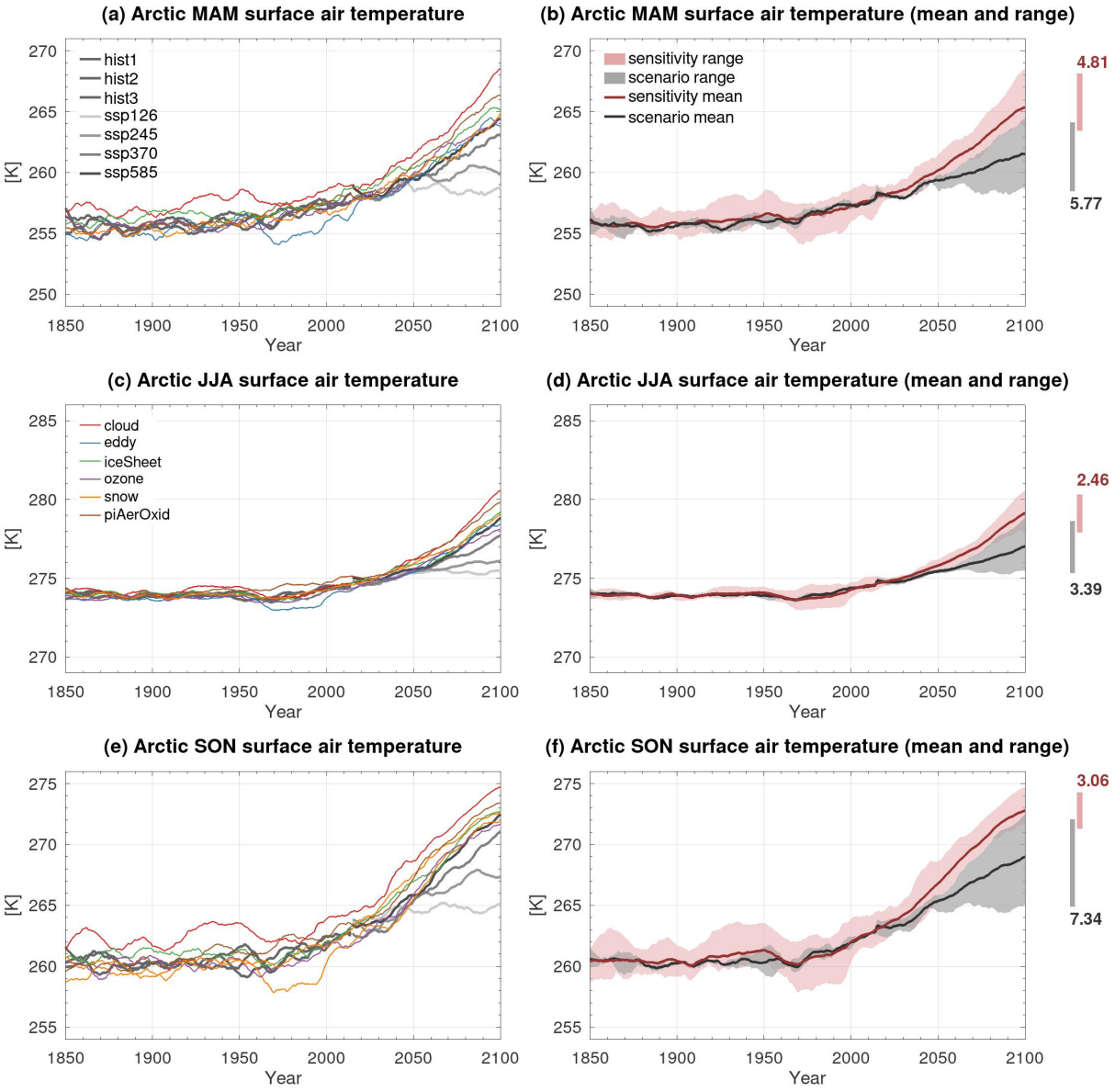

Figure S1. Time evolution of spring (March–May; MAM; a–b), summer (June–August; JJA; c–d), and fall (September–November; SON; e–f) Arctic surface temperature for 1850–2100. In a, c, and e, the individual lines show the CMIP6 historical realizations (hist1, hist2, and hist3), four future scenarios (ssp126, ssp245, ssp370, ssp585), and the six sensitivity experiments (*cloud*, *eddy*, *iceSheet*, *ozone*, *snow*, and *piAerOxid*). In b, d, and f, the lines show the mean warming for the scenarios (grey) and sensitivity experiments (red) and the shading shows the warming range between the experiments with strongest and weakest warming. To highlight the end-of-the-century warming range, the difference between the experiment with strongest and weakest warming in 2100 is additionally shown in terms of the numbers and vertical bars to the right of b, d, and f. A 10-year running mean has been applied. Units are in K.

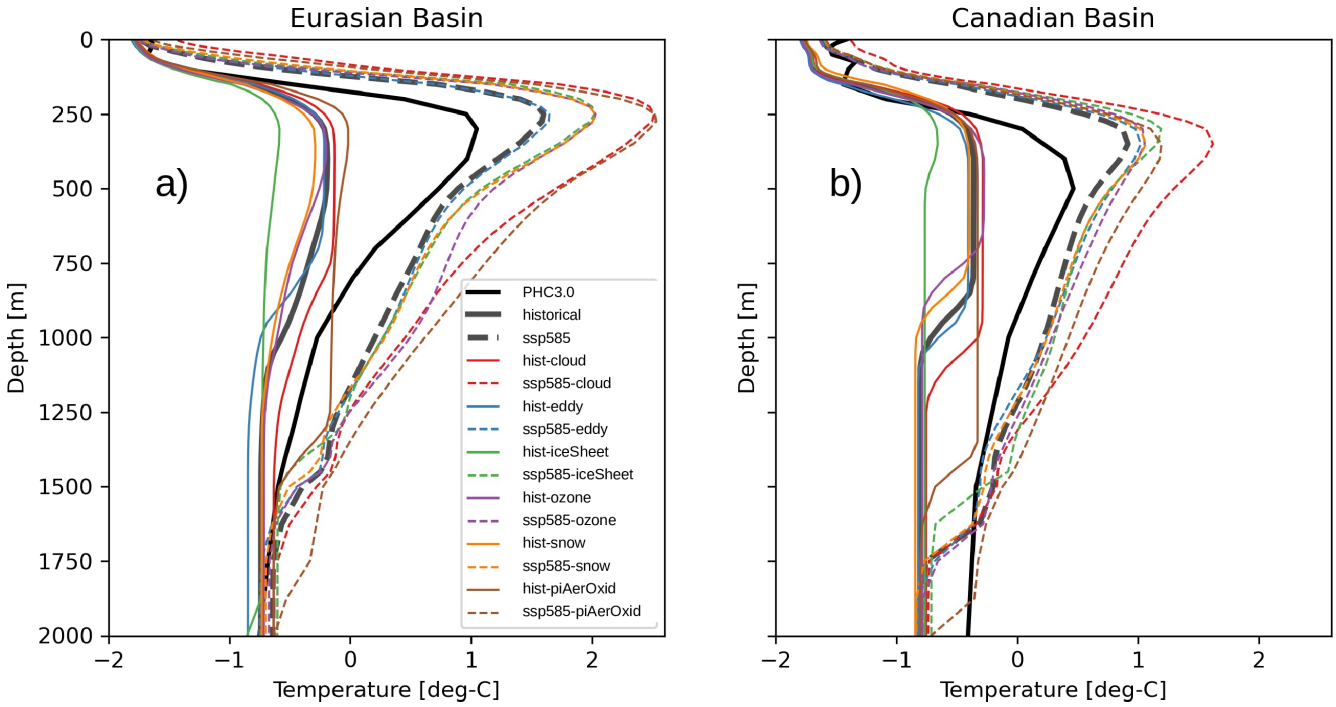

Figure S2. Historical (solid lines) and future (dashed lines) vertical ocean temperature profiles averaged for the Eurasian (a) and Canadian Basins (b). Both panels show the historical and ssp585-based experiments for the baseline (historical and ssp585; grey lines), *cloud* (hist-cloud and ssp585-cloud; red lines), *eddy* (hist-eddy and ssp585-eddy; blue lines), *iceSheet* (hist-iceSheet and ssp585-icesheet; green lines), *ozone* (hist-ozone and ssp585-ozone; purple lines), *snow* (hist-snow and ssp585-snow; orange lines), and *piAerOxid* (hist-piAerOxid and ssp585-piAerOxid; brown lines) experiments. Observations (black solid lines) are from the Polar Science Center Hydrographic Climatology (PHC Steele et al., 2001) version 3.0. Units are in C.

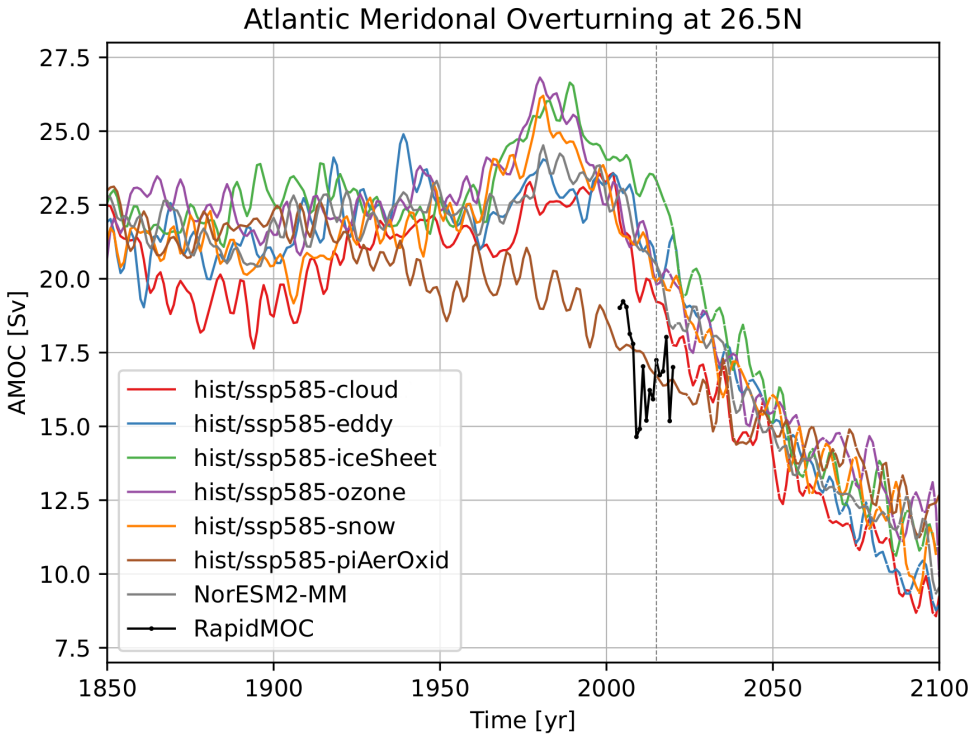

Figure S3. Time evolution of the Atlantic meridional overturning circulation at 26.5 N for the baseline (historical and ssp585; grey line) *cloud* (hist-cloud and ssp585-cloud; red line), *eddy* (hist-eddy and ssp585-eddy; blue line), *iceSheet* (hist-iceSheet and ssp585-iceSheet; green line), *ozone* (hist-ozone and ssp585-ozone; purple line), *snow* (hist-snow and ssp585-snow; orange line), and *piAerOxid* (hist-piAerOxid and ssp585-piAerOxid; brown line) experiments. Also shown is the RapidMOC estimate (black line; McCarthy et al., 2015). Units are in Sv.

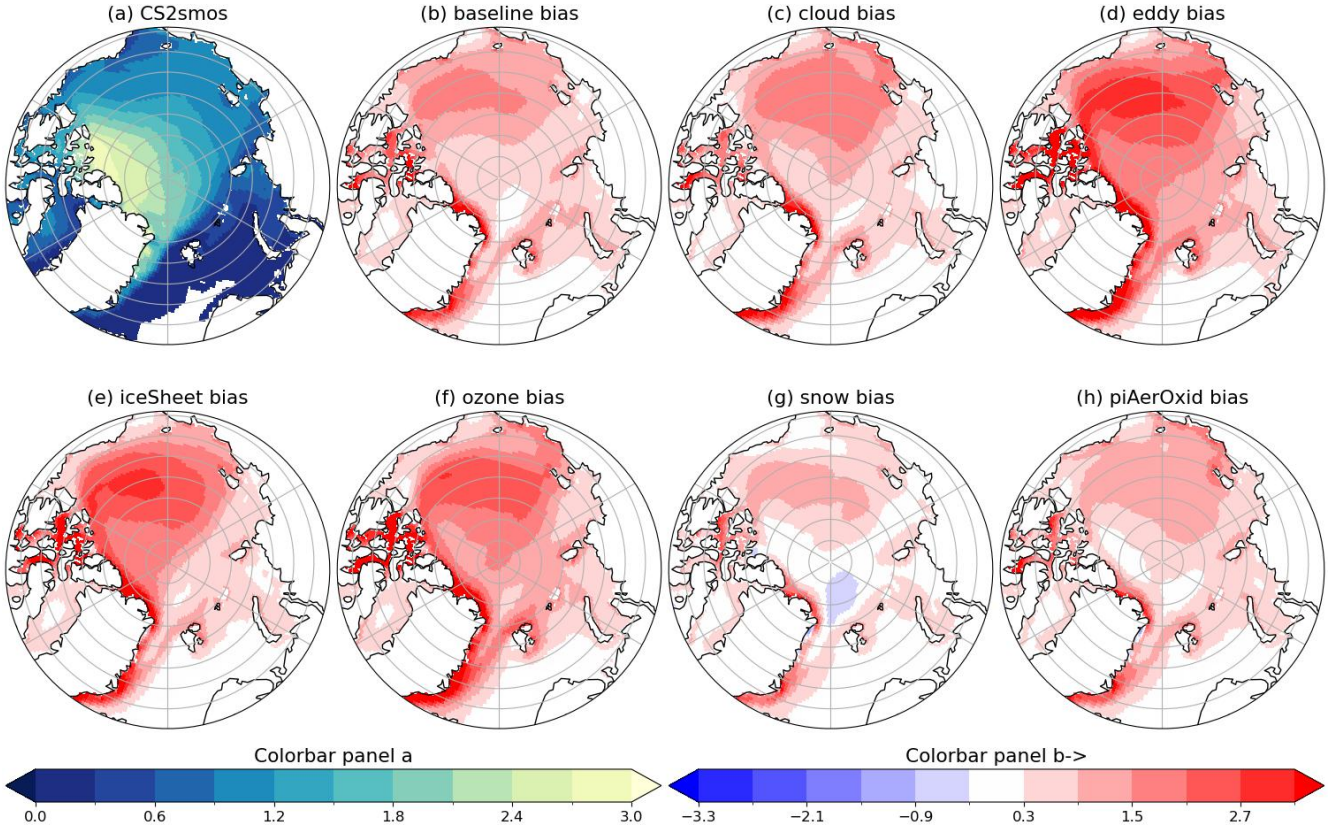

Figure S4. Spatial distribution of observed winter (December–February; DJF) sea-ice volume from CryoSat-2 – SMOS for the period 2011–2022 (a), and the bias in sea-ice volume with respect to the observations for the historical baseline (b), *cloud* (c), *eddy* (d), *iceSheet* (e), *ozone* (f), *snow* (g), and *piAerOxid* experiments (h). The model climatologies are based on years 2011–2014 from the historical experiments and years 2015–2022 from the ssp585 experiments. Units are in thickness per unit area.